Biochemical and Biophysical Research Communications 452 (2014) 443–449

Contents lists available at ScienceDirect

Biochemical and Biophysical Research Communications

journal homepage: www.elsevier.com/locate/ybbrc

Structural and functional studies of conserved nucleotide-binding protein *LptB* in lipopolysaccharide transport

Zhongshan Wang [a,b,c,1], Quanju Xiang [b,c,d,1], Xiaofeng Zhu [b], Haohao Dong [c], Chuan He [e], Haiyan Wang [b], Yizheng Zhang [b], Wenjian Wang [f,*], Changjiang Dong [a,*]

[a] Biomedical Research Centre, Norwich Medical School, University of East Anglia, Norwich Research Park, NR4 7TJ, UK
[b] College of Life Sciences, Sichuan University, Chengdu 610065, China
[c] Biomedical Sciences Research Complex, School of Chemistry, University of St Andrews, North Haugh, St Andrews KY16 9ST, UK
[d] Department of Microbiology, College of Resource and Environment Science, Sichuan Agriculture University, Yaan 625000, China
[e] School of Electronics and Information, Wuhan Technical College of Communications, No. 6 Huangjiahu West Road, Hongshan District, Wuhan, Hubei 430065, China
[f] Laboratory of Department of Surgery, The First Affiliated Hospital, Sun Yat-sen University, 58 Zhongshan Road II, Guangzhou, Guangdong 510080, China

ARTICLE INFO

Article history:
Received 18 August 2014
Available online 27 August 2014

Keywords:
Lipopolysaccharide transport protein
Gram-negative bacteria
LptB
Nucleotide-binding protein
Crystal structure and function

ABSTRACT

Lipopolysaccharide (LPS) is the main component of the outer membrane of Gram-negative bacteria, which plays an essential role in protecting the bacteria from harsh conditions and antibiotics. LPS molecules are transported from the inner membrane to the outer membrane by seven LPS transport proteins. LptB is vital in hydrolyzing ATP to provide energy for LPS transport, however this mechanism is not very clear. Here we report wild-type LptB crystal structure in complex with ATP and Mg^{2+}, which reveals that its structure is conserved with other nucleotide-binding proteins (NBD). Structural, functional and electron microscopic studies demonstrated that the ATP binding residues, including K42 and T43, are crucial for LptB's ATPase activity, LPS transport and the vitality of *Escherichia coli* cells with the exceptions of H195A and Q85A; the H195A mutation does not lower its ATPase activity but impairs LPS transport, and Q85A does not alter ATPase activity but causes cell death. Our data also suggest that two protomers of LptB have to work together for ATP hydrolysis and LPS transport. These results have significant impacts in understanding the LPS transport mechanism and developing new antibiotics.

1. Introduction

Lipopolysaccharide (LPS) is a main component of the outer membrane of Gram-negative bacteria, which is essential for the vitality of most Gram-negative bacteria, playing crucial roles in forming a biofilm and protecting the organisms from harsh environments [1]. Seven of the lipopolysaccharide transport proteins, namely LptA, B, C, D, E, F and G, form a trans-envelope complex for LPS transport from the inner membrane to the outer leaflet of the outer membrane, of which the LptBFG proteins form an ABC transporter that extracts LPS from the inner membrane and passes it to the inner membrane protein LptC which then delivers it to the LptA [2,3]. LptA transports LPS to the outer membrane LPS translocon LptD/E complex, in which the LPS is inserted into the outer membrane [4,5]. Two crystal structures of LptD/E complex from *Salmonella typhimurium LT12* and *Shigella flexneri* were reported, and both structures revealed that the LptD/E forms a novel two-protein "barrel and plug" architecture, with the LptD forming a 26-stranded barrel [6,7]. Our functional assays and molecular dynamics simulations suggested that LptD inserts LPS into the outer membrane through a lateral opening between strands β1 and β26 [6].

The outer membrane of a single *Escherichia coli* cell has around 2×10^6 LPS molecules and all the LPS molecules have to be transported to the outer leaflet of the outer membrane from the inner membrane. LptB hydrolyzes ATP to provide the energy for LPS transport [5]. Unlike previous reported ABC transporters, LptBCFG does not transport the LPS across the inner membrane but extracts the LPS directly from the inner membrane instead [8,9]. LptB is a potential drug target for development of novel drugs; however, work is hampered as there is no structure available for rational drug design [10,11]. While preparing this manuscript, structures describing an inactive LptB in complex with ATP, and LptB with ADP were published [12] in which three residues (E163, H195 and F90) have been identified to be essential for the LPS transport,

* Corresponding authors.
E-mail addresses: Wenjian166@gmail.com (W. Wang), C.Dong@uea.ac.uk (C. Dong).
[1] These authors contributed equally to this work.

http://dx.doi.org/10.1016/j.bbrc.2014.08.094
0006-291X/

although the H195 and F90 mutations did not significantly decrease LptB's ATPase activity. The studies, however, did not show how the substrate binding residues affected ATPase activity and LPS transport, which is crucial not only for understanding the transport mechanism but also important for rational drug design. Here, we report the wild-type LptB protein structure in complex with ATP and Mg^{2+}; we systematically generated alanine substitutions of the active site residues and performed *in vitro* and *in vivo* assays to further understand the relationship between ATPase activity and LPS transport. Particularly, we demonstrated that residues S139 and E142 of another protomer in the LptB dimer are essential for the LptB's ATPase activity and cell vitality. Finally, we have examined the ultrastructure of H195A mutant strain using transmission electron microscopy.

2. Materials and methods

2.1. Plasmid constructions

The *E. coli lptB* gene was amplified by PCR using genomic *E. coli* K12 DNA and introduced into the hexahistidine (6×His) tag at the C-terminus of LptB into plasmid pACYCDuet (Novagen). All the *lptB* mutations of the active site residues were generated using site-directed mutagenesis kits (Stratagene) according to the manufacturer's instruction. The primers used in the cloning and mutagenesis are shown in Supplementary Table 1. All *lptB* constructs were confirmed by DNA sequencing.

2.2. Protein expression and purification

BL21(DE3) cells containing lptB plasmids were grown at 37 °C in Terrific Broth containing 34 μg/mL chloramphenicol (Chl). Expression was induced by adding 0.15 mM IPTG for 16 h at 25 °C, when OD_{600} of the cell cultures reached ~0.6. The cells were harvested by centrifugation at 5000*g* for 15 min and the pellets were resuspended in 20 mM Tris–HCl, pH 7.5, 10% (v/v) glycerol, 5 mM $MgCl_2$ and 2 mM ATP containing 1 mM phenylmethylsulfonyl fluoride (PMSF, Sigma), 50 μg/mL DNase I (Sigma) and 1 protease inhibitor tablet (Roche). Cells were disrupted by a French Press (Thermo Electron). The cell lysate was centrifuged at 15,000*g* for 30 min and the supernatant was loaded onto nickel-nitrilotriacetic acid (Ni-NTA) beads (Qiagen) and washed with 20 mM Tris–HCl, pH7.5, 0.3 M NaCl and 30 mM imidazole. LptB was eluted with 20 mM Tris–HCl, pH 7.5, 0.3 M NaCl and 300 mM imidazole. The protein was further purified by a size exclusion column Superdex-200 with 20 mM Tris–HCl, pH 7.5, 0.5 M NaCl and 5% (v/v) glycerol. The protein was confirmed by mass spectrometry. All the mutants of LptB were overexpressed and purified similarly.

2.3. LptB crystallization

Purified *LptB*-6×His was concentrated to 10 mg/mL. 2 mM ATP and 5 mM $MgCl_2$ were added to the protein before crystallization. The diamond-shaped crystals grew in 1 week in 0.2 M ammonium fluoride and 20% PEG 3350 at 20 °C, using the sitting-drop vapor diffusion method with 0.5 μL of protein and 0.5 μL of the crystallization solution.

2.4. Data collection and structure determination

LptB-6×His crystals were cryo-protected by a solution containing 20% PEG 3350, 0.2 M ammonium fluoride and 20% glycerol, and flash-cooled in liquid nitrogen prior to data collection at IO4-1 of the Diamond Light Source, UK. The data was indexed and integrated using Mosflm [13], and scaled using SCALA [14]. The structure was determined by molecular replacement using Phenix [15]. The model was built using Phenix and Coot [16], and structural refinements were performed with REFMAC5 [17].

2.5. LptB ATPase activity determination

LptB ATPase activity was determined using a revised method [15]. Briefly, the reaction was carried out in 20 mM Tris–HCl, pH 7.5, 0.5 M NaCl and 5% (v/v) glycerol, containing 0.8 μM wild-type or mutant *LptB*-6×His, 0.1 mg/mL BSA, 5 mM $MgCl_2$, 6 units/mL pyruvate kinase, 0.1 unit/mL lactate dehydrogenase, 4 mM phospho(enol) pyruvic acid and 0.32 mM β-Nicotinamide adenine dinucleotide, reduced dipotassium (NADH). The reactions were initiated by adding 1 mM ATP. NADH oxidation was measured by recording the changes in absorbance at 465 nm (λex = 340 nm, λem = 465 nm) with a Nanodrop. Known concentrations of NADH in the reaction buffer were used to generate a standard curve; the error bars represent the mean ± SD (n = 3).

2.6. In vivo LptB functional assays

The plasmids encoding LptB-6×His and mutants were introduced into BB-5 cells for the functional assay. BB-5 is an *lptB* depletion strain derived from *E. coli* BW25113, in which the inducible *araBp* promoter controls the expression of the *lptB* genes [18]. All the mutant strains were cultured in LB (34 μg/mL kan, 34 μg/ml chl and 0.2% arabinose) overnight at 37 °C. 0.5 mL of these overnight cultures were pelleted, washed twice with LB broth, and diluted 1000-fold into fresh LB broth (34 μg/mL kan, 34 μg/mL chl and 0.1 M IPTG for all the transformants). A control was also prepared where the BB-5 strain was diluted 1000-fold in LB with 0.2% arabinose (ara^+) or without arabinose (ara^-). After 2 h, *E. coli* cell growth was monitored by measuring the OD_{600} of the cultures at hourly intervals for 7 h.

2.7. Electron microscopy

Bacterial samples for Transmission Electron Microscopy (TEM) were prepared according to a reported method [18]. Cultures from above were collected by centrifugation when the growth curve started falling (at approximately 6 h). The pellets were washed and resuspended in PBS (pH 7.4). Thin 70-nm sections were obtained using a diamond knife on a Leica UC6 Ultramicrotome, and observed on a tecnai G2 F20 (FEI, USA) Transmission Electron Microscope equipped with an Omega Energy Filter. Micrographs were taken directly under the microscope with Kodak 4489 photographic films for TEM.

3. Results

3.1. The structure of LptB

The crystals belong to space group $C222_1$ with cell dimensions a = 85.16 Å, b = 125.76 Å, c = 89.61 Å and $\alpha = \beta = \gamma = 90°$ (Supplementary Table 2). The structure of LptB was determined to 2.22-Angstrom resolution by molecular replacement using Phenix, and an ATP-binding subunit of a branched amino acid ABC transporter (1JI0) from *Thermotoga maritima* as a search model. There are two LptB protomers in an asymmetric unit. The model contains residue A2 to G236. LptB comprises ten α-helixes and ten β-sheets, forming two domains; the RecA-like domain and α-helical domain (Fig. 1A and B). Between the two domains, there is a highly hydrophobic groove, which we predict to be binding sites of the transmembrane domains of LptF and G (more details in Section 4) (Fig. 1C and D).

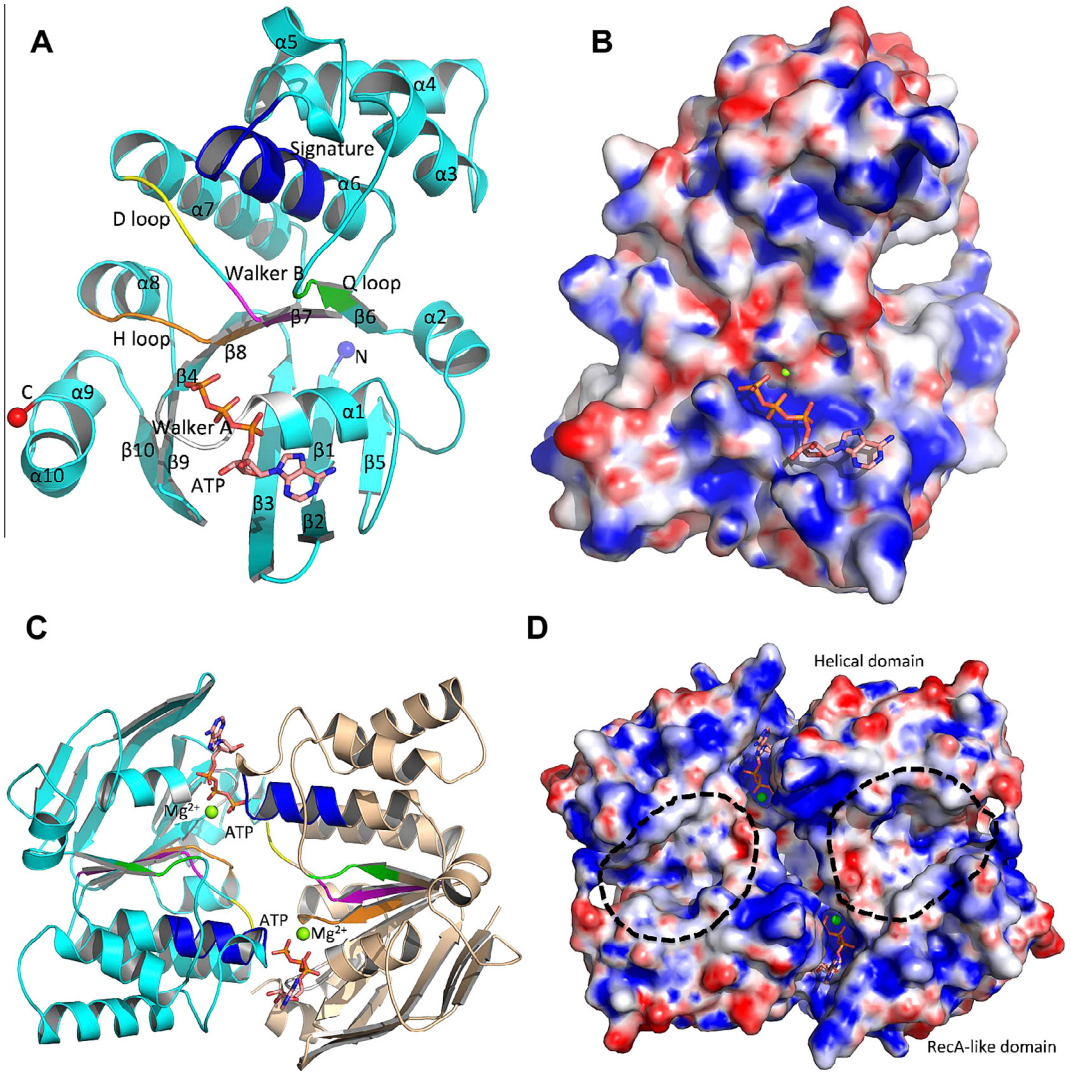

Fig. 1. Structure of LptB. The ATP molecule is shown in stick. (A) Carton representation of a protomer structure of LptB in cyan. The Walker A motif, H-loop, Walker B motif, D-loop, Q-loop and signature motif are in gray, orange, magentas, yellow, green and blue, respectively. (B) Potential electrostatic map of LptB protomer. Negative charged residues in red and positive charged residues in blue. (C) Dimeric structure of LptB in cartoon. The ATP molecules are located between two protomers. One protomer in cyan and another in gray. The motifs are in the same colors as in (A). (D) Potential electrostatic map of the dimeric LptB. There are grooves between the helical and the RecA-like domains (shown in dark dotted circles), which is highly hydrophobic, which is potential sites to host the "coupling domains" of the transporter's transmembrane domains. (For interpretation of the references to color in this figure legend, the reader is referred to the web version of this article.)

LptB's structure is very conserved, having the Walker A, Walker B, Q-loop, D-loop, H-loop and ABC signature motifs (Fig. 1A), which are the features of NBDs [19,20].

3.2. ATP locates into the active site of LptB

There are clear electron densities for two ATP molecules and two Mg^{2+} ions in the asymmetric unit, indicating that each LptB molecule is bound to one ATP molecule and one Mg^{2+} ion (Fig. 2A). The explanation as to why ATP, but not ADP presents in the structure is that ammonium fluoride could inhibit the reaction. The adenine of ATP is stocked against the hydrophobic side chain Y13, while the ribose is anchored by R16 and V18. The α-phosphate interacts with the side chain of T44, whereas β-phosphate forms a salt bridge with the side chain of K42 and interacts with the main chains of the Walker A loop. The γ-phosphate is anchored extensively by side chains N38, K42 of the Walker A motif, Q85 of the Q-loop, E163 of the Walker B, H195 of the H-loop. The Mg^{2+} ion is coordinated by β-phosphate, γ-phosphate, Q85, T43, and two water molecules (Wat1 and Wat2) (Fig. 2A). Sequence alignment shows that residues N38, K42, T43, T44, Q85, E163 and H195 from the typical motifs involved in the ATP binding and hydrolysis are absolutely conserved, while residues Y13, R16, and V18 are highly conserved (Supplementary Fig. 1). E163 is proposed as a catalytic base for activation of a water molecule for the hydrolysis of the ATP but the functions of other residues in the catalytic reaction are debatable [19,20]. Collectively, LptB forms a highly charged pocket with hydrophobic patches for substrate ATP binding (Figs. 1B and 2A).

3.3. LptB forms dimers in solution

Size-exclusion chromatography of LptB suggested that it is dimeric in solution when ATP is present, which is consistent with other NBDs [21,22]. The dimeric structure of LptB is generated according to symmetry-related molecules. The ATP is sandwiched by two subunits of LptB, where the ATP is between the RecA-like domain (Walker A) of one subunit and the signature motif of another subunit in a head-to-tail arrangement. The E142 and

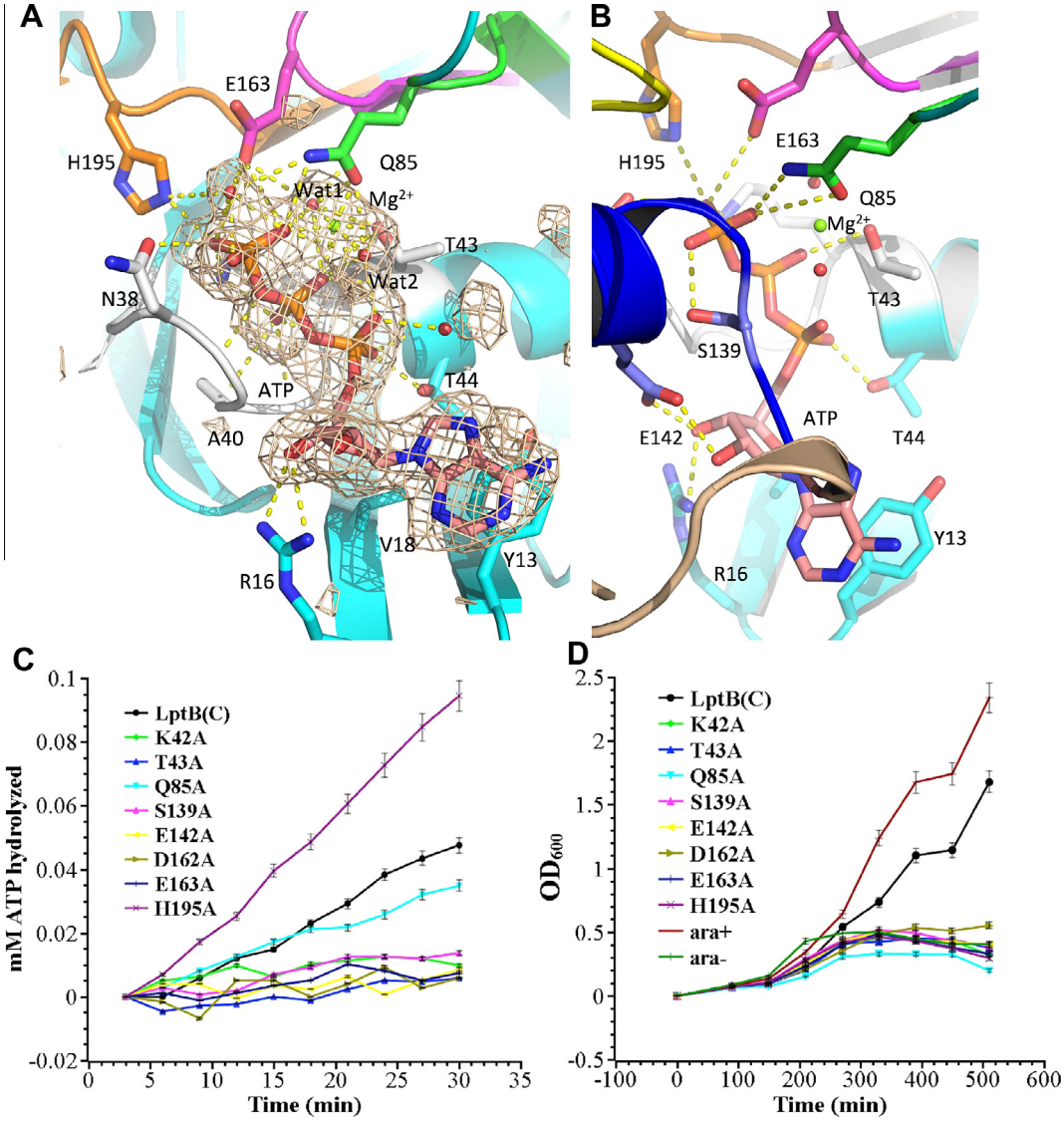

Fig. 2. LptB active site residues and their importance for ATPase activity and the vitality of the *E. coli* cells. (A) ATP molecule is located into the active site, which interacts with residues Y13, R16, N38, H195, E163, Q85, T43, T44 and V18. The Mg^{2+} ion is coordinated by phosphates of ATP, water molecules, E163 and T43. An unbiased FoFc electron density map of ATP is shown at 2.5 σ. (B) Residues S139 and E142 from signature motif of another protomer interact with the ATP molecule. (C) ATPase activity of the LptB variants. The ATPase activity of H195A increases and Q85A is very similar to LptB-6×His, while other variants K42A, D162A, E163A, S139A and E142A significantly decrease the ATPase activity. The error bars represent the mean ± SD (n = 3). (D) LptB variants result in *E. coli* cell deaths. All mutations cause the cell deaths, which showed the discrepancy between the ATPase activity and cell vitality, particular mutation H195A, and Q85A. The error bars represent the mean ± SD (n = 3).

S139 from the signature motif interact with the ribose and the γ-phosphate of the ATP, respectively (Figs. 1C, D and 2B).

3.4. The potential active site residues are crucial for ATPase activity

To check whether these active site residues are essential for *in vitro* activity, we generated the alanine substitutions K42A, T43A, Q85A, S139A, E142A, D162A, E163A and H195A with C-terminal 6×His tag. We performed *in vitro* assays to test the ATPase activities of the variants (Fig. 2C), and we adjusted all mutant protein samples to the same concentration. The E163A variant showed no activity, which is consistent with the essential role of E163 as catalytic residue in the NBDs [21,22]. Surprisingly, the H195A mutant showed greater activity than wild-type *LptB*-6×His, contrary to other known NBDs where such a mutation resulted in a total loss of activity [21,22]. The Q85A variant in the Q-loop showed similar activity to wild-type LptB-6×His, which is different from other NBDs where such a mutation significantly decreased ATPase activities [21,22], while mutants K42A, T43A, and S139A significantly lowered ATPase activity. Beside for the H195A and Q85A variant, these activity data suggest that residues E142, S139, D162, and E163 from the conserved motifs are essential for LptB activity (Fig. 2C). Importantly, we have also proven that residues K42 and T43 from the non-conserved motifs are also essential for ATPase activity.

3.5. The ATP binding residues are essential for the vitality of E. coli cells

To test whether the active site residues are important for the *E. coli* cell growth, we transformed the plasmids encoding wild-type and mutant variants of *lptB* into *lptB* depleted *E. coli* BB-5 cells. The BB-5 cells with the *LptB*-6×His plasmid could grow in LB medium when induced with 0.1 mM IPTG (Fig. 2D). BB-5 cells bearing K42A, T43A, S139A, E142A, D162A, and E163A mutant expressing plasmids showed significantly impaired cell growths (Fig. 2D), which is consistent with the *in vitro* assays where these mutations

showed a loss of ATPase activity (Fig. 2C). These results strongly suggest that the ATPase activity of LptB is crucial for the vitality of *E. coli* cells. However, there are two exceptions; one is the H195A mutant which was found to have greater activity than *LptB*-6×His *in vitro*, but caused *E. coli* death *in vivo*; the second is the Q85A mutant which showed comparable activity to wild-type LptB *in vitro,* but resulted in cell death *in vivo*. The explanation of the differences between the *in vitro* and *in vivo* assays of H195A and Q85A could be because of differing protein expression levels of the two variants in the membrane, or differing protein–protein interactions in forming the ABC transporters [12].

3.6. LptB mutant impairs LPS transport in E. coli

It is reported that the morphological and structural abnormalities of *E. coli* cells in *lptA*, *B*, *C*, *D*, *E*, *F* and *G* depletion strains, are the result of blocked LPS transport to the outer leaflet of the outer membrane [18,23]. To check whether the *lptB* variants can stop LPS transport, we performed TEM studies of the BB-5 *E. coli* cells with the H195A mutant and the *E. coli* cells expressing wild-type LptB-6×His (Fig. 3A and B). The H195A mutant showed fiber-like cells with membrane accumulation in the periplasm, or budding of vesicles from the outer membrane, which is a typical phenotype of *lptB* depletion strains that is different from the wild-type [18], indicating that the LPS molecules have not been delivered to the outer membrane correctly.

4. Discussion

Proteins LptB, C, F and G form a unique ABC transporter to extract LPS molecules from the inner membrane, where the transporter is powered by LptB hydrolyzing ATP [5,24]. We report here the wild-type LptB structure in complex with ATP and Mg^{2+} ion, which revealed the critical residues in ATP binding and hydrolysis. The mutagenesis studies, *in vitro* ATPase assays and *in vivo* cell growth assays confirmed the characteristics of LptB's key ATPase sites. Unlike other NBDs, the Q85A mutation did not result in a decrease in ATPase activity, but resulted in cell death (Fig. 2C and D). The H195A mutant showed an increase in ATPase activity *in vivo*, but caused cell death *in vivo*, and defective LPS transport (Fig. 2C and D). These results may reflect characteristics that distinguish LptB from other NBDs, where LptB may behave differently when isolated from the entire LptBCFG transporter in the cell membrane. This suggests that we should combine the *in vitro* and *in vivo* assays together for drug discovery studies. We also performed systemic *in vitro* ATPase activity and *in vivo* cell growth assays with mutants E163A, S139A, E142A and D162A, K42A and T43A of the conserved residues, which showed that these variants significantly impair ATPase activity and cell growth. It is important to mention that S139 and E142 are involved in the ATP binding from another protomer of the dimer, and that mutants S139A and E142A resulted in a decrease of LptB activity and caused the deaths of the BB-5 cells, strongly suggesting that the two protomers of the LptB dimer have to work together for ATP hydrolysis, which could provide the energy to drive the rotation of the α-helical domains of LptB. This could lead to conformational changes in the transmembrane domains to extract LPS from the inner membrane. Altogether, these results may help to expand our understanding of the critical biological processes of LPS transport and assist rational drug design.

The structure of LptB resembles the NBD of maltose transporter (2R6G) with Root-square deviation (RMSD) of 1.581 over 223 Cα atoms, and those of other type I transporters (Fig. 4A). However, NBDs of type I transporters normally have three domains, the α-helical domain, the RecA-like domain and the regulation domain. The structure of LptB resembles the NBD of vitamin B12 transporter (2QI9) with RMSD of 1.777 over 214 Cα atoms (Fig. 4B). The vitamin B12 transporter is a type II transporter, and the NBD comprises only two domains, the α-helical domain and the RecA-like domain.

When superimposed, the structure of dimeric LptB against subunit BtuD of the vitamin B transporter (BtuCDF, 2QI9), revealed that the dimeric arrangement of the two NBDs is very similar, including the way the ATPs bind (Fig. 2B). The superimposition also revealed that the two grooves between the RecA-like domain and the α-helical domain of the LptB are potential transmembrane domain binding sites, where the grooves could host the "coupling helices" from the transmembrane domains of the transporter (Fig. 4B and C). Each groove comprises highly hydrophobic residues I52, L72, H73, Y82, P84, F90, V102, and I105. We postulate that hydrolysis of ATP and the release of ADP would result in significant conformational changes of LptB, which will cause the conformational changes of the transmembrane domains of LptF and LptG. These conformational changes may laterally open a gate between the LptF and LptG to extract the LPS from the inner membrane. The LptB not only provides the energy for LptBCFG to extract the LPS from the inner

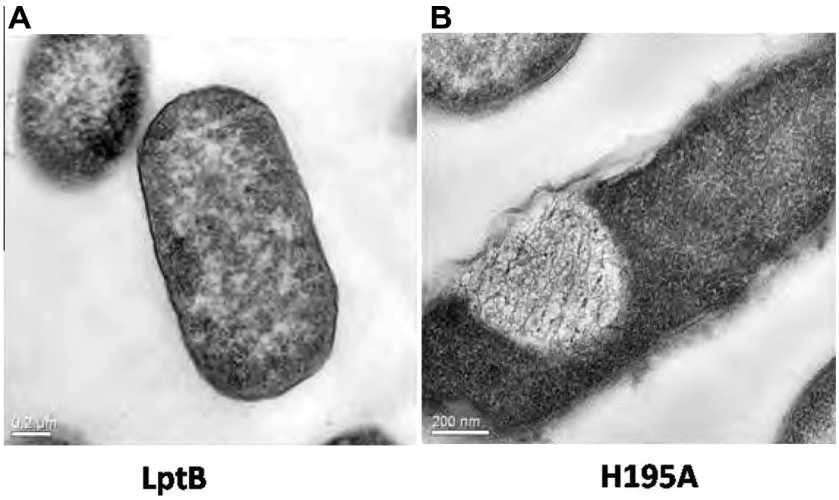

Fig. 3. Morphological abnormity of LptB variants. (A) The BB-5 cells with the LptB-6×His. (B) The BB-5 cells with H195A of LptB-6×His. The cells become fiber-like shape with membrane accumulation, which is very similar to LptB depletion strain.

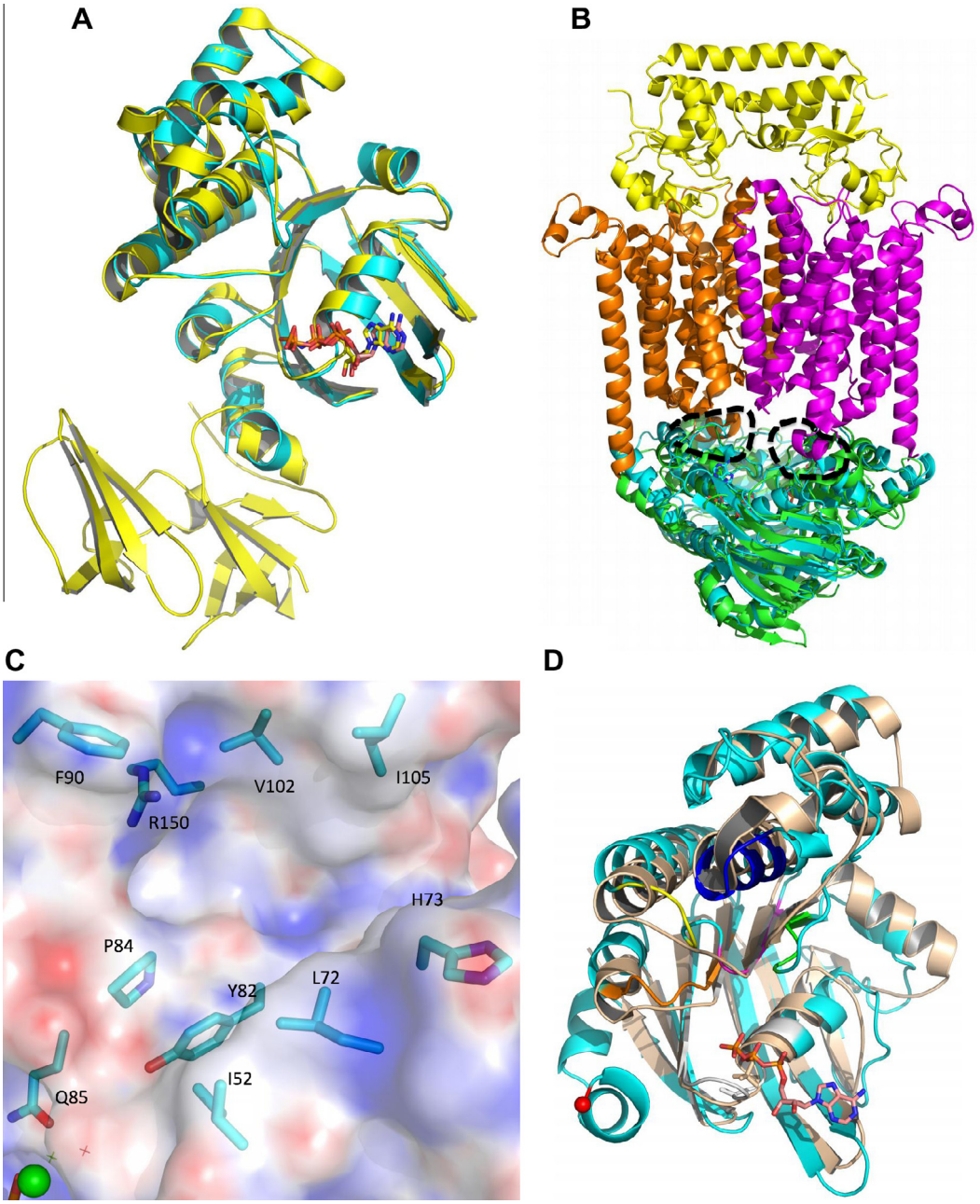

Fig. 4. LptB structure is similar to other NBDs of transporters. The LptB is in cyan, while NBD domains of BtuBCD and LolCDE are colored in green and gray, respectively. (A) LptB structure is superimposable to that of NBD domain of the maltose transporter. The NBD of the maltose transporter has additional regulatory domain. (B) LptB is superimposed to NBD domain of vitamin B12 transporter, suggesting that the groves between the α-helical and RecA-like domains are potential sites for hosting the "coupling helices" of the transmembrane domains. (C) The potential residues may involve in binding the LptB to the transmembrane domains. (D) LptB is superimposed to NBD of LolCDE, which is responsible for lipoprotein transport. (For interpretation of the references to color in this figure legend, the reader is referred to the web version of this article.)

membrane, but also provides the energy for the LPS transfer from LptC to LptA, indicating that the LptBCFG transporter may be quite a unique example of a type II transporter [5]. Furthermore, LptB's structure is very similar to that of the NBD of LolCDE (Fig. 4D), indicating that LolCDE may use mechanism similar to LptBCFG for extracting lipoproteins from the inner membrane.

5. Protein Data Bank accession code

The structure factor and coordinates of LptB in complex with ATP and magnesium ions are deposited in the Protein Data Bank at accession code 4QC2.

Acknowledgments

The work is supported by Wellcome Trust career development fellowship to C.J.D. (WT083501MA) and the Natural Science Foundation of Guangdong Province, China to W.J.W (S2013010016539). We thank the staff of the I04-1 beam station at the Diamond Light Source UK for their assistance in data collection, and Prof. Gianni Deho for the *LptB* depleted BB-5 cells.

Appendix A. Supplementary data

Supplementary data associated with this article can be found, in the online version, at http://dx.doi.org/10.1016/j.bbrc.2014.08.094.

References

[1] C. Whitfield, M.S. Trent, Biosynthesis and export of bacterial lipopolysaccharides, Annu. Rev. Biochem. 83 (2014) 1–30.

[2] Q. Xiang, H. Wang, Z. Wang, Y. Zhang, C. Dong, Characterization of lipopolysaccharide transport protein complex, Cent. Eur. J. Biol. 9 (2014) 131–138.

[3] G. Chimalakonda, N. Ruiz, S.-S. Chng, R.A. Garner, D. Kahne, T.J. Silhavy, Lipoprotein LptE is required for the assembly of LptD by the beta-barrel assembly machine in the outer membrane of *Escherichia coli*, Proc. Natl. Acad. Sci. USA 108 (2011) 2492–2497.

[4] P. Sperandeo, F.K. Lau, A. Carpentieri, C. De Castro, A. Molinaro, G. Deho, T.J. Silhavy, A. Polissi, Functional analysis of the protein machinery required for transport of lipopolysaccharide to the outer membrane of *Escherichia coli*, J. Bacteriol. 190 (2008) 4460–4469.

[5] S. Okuda, E. Freinkman, D. Kahne, Cytoplasmic ATP hydrolysis powers transport of lipopolysaccharide across the periplasm in *E. coli*, Science 338 (2012) 1214–1217.

[6] H. Dong, Q. Xiang, Y. Gu, Z. Wang, N.G. Paterson, P.J. Stansfeld, C. He, Y. Zhang, W. Wang, C. Dong, Structural basis for outer membrane lipopolysaccharide insertion, Nature 511 (2014) 52–56.

[7] S. Qiao, Q. Luo, Y. Zhao, X.C. Zhang, Y. Huang, Structural basis for lipopolysaccharide insertion in the bacterial outer membrane, Nature 511 (2014) 108–111.

[8] R.N. Hvorup, B.A. Goetz, M. Niederer, K. Hollenstein, E. Perozo, K.P. Locher, Asymmetry in the structure of the ABC transporter-binding protein complex BtuCD-BtuF, Science 317 (2007) 1387–1390.

[9] M.L. Oldham, J. Chen, Crystal structure of the maltose transporter in a pretranslocation intermediate state, Science 332 (2011) 1202–1205.

[10] D.J. Sherman, S. Okuda, W.A. Denny, D. Kahne, Validation of inhibitors of an ABC transporter required to transport lipopolysaccharide to the cell surface in *Escherichia coli*, Bioorg. Med. Chem. 21 (2013) 4846–4851.

[11] L.S. Gronenberg, D. Kahne, Development of an activity assay for discovery of inhibitors of lipopolysaccharide transport, J. Am. Chem. Soc. 132 (2010) 2518–2519.

[12] D.J. Sherman, M.B. Lazarus, L. Murphy, C. Liu, S. Walker, N. Ruiz, D. Kahne, Decoupling catalytic activity from biological function of the ATPase that powers lipopolysaccharide transport, Proc. Natl. Acad. Sci. USA 111 (2014) 4982–4987.

[13] A.G.W. Leslie, H.R. Powell, Processing diffraction data with MOSFLM, Nato. Sci. Ser. II. Math. 245 (2007) 41–51.

[14] P. Evans, Scaling and assessment of data quality, Acta Cryst. D62 (2006) 72–82.

[15] P.D. Adams, P.V. Afonine, G. Bunkoczi, V.B. Chen, I.W. Davis, N. Echols, J.J. Headd, L.W. Hung, G.J. Kapral, R.W. Grosse-Kunstleve, A.J. McCoy, N.W. Moriarty, R. Oeffner, R.J. Read, D.C. Richardson, J.S. Richardson, T.C. Terwilliger, P.H. Zwart, PHENIX: a comprehensive Python-based system for macromolecular structure solution, Acta Cryst. D66 (2010) 213–221.

[16] P. Emsley, B. Lohkamp, W.G. Scott, K. Cowtan, Features and development of Coot, Acta Cryst. D66 (2010) 486–501.

[17] G.N. Murshudov, A.A. Vagin, E.J. Dodson, Refinement of macromolecular structures by the maximum-likelihood method, Acta Cryst. D53 (1997) 240–255.

[18] P. Sperandeo, R. Cescutti, R. Villa, C. Di Benedetto, D. Candia, G. Deho, A. Polissi, Characterization of lptA and lptB, two essential genes implicated in lipopolysaccharide transport to the outer membrane of *Escherichia coli*, J. Bacteriol. 189 (2007) 244–253.

[19] E. Biemans-Oldehinkel, M.K. Doeven, B. Poolman, ABC transporter architecture and regulatory roles of accessory domains, FEBS Lett. 2006 (580) (2006) 1023–1035.

[20] K. Hollenstein, R.J. Dawson, K.P. Locher, Structure and mechanism of ABC transporter proteins, Curr. Opin. Struct. Biol. (2007) 412–418.

[21] N. Tal, E. Ovcharenko, O.A. Lewinson, Single intact ATPase site of the ABC transporter BtuCD drives 5% transport activity yet supports full in vivo vitamin B12 utilization, Proc. Natl. Acad. Sci. USA 110 (2013) 5434–5439.

[22] J. Zaitseva, S. Jenewein, T. Jumpertz, I.B. Holland, L. Schmitt, H662 is the linchpin of ATP hydrolysis in the nucleotide-binding domain of the ABC transporter HlyB, EMBO J. 24 (2005) 1901–1910.

[23] N. Ruiz, L.S. Gronenberg, D. Kahne, T.J. Silhavy, Identification of two inner-membrane proteins required for the transport of lipopolysaccharide to the outer membrane of *Escherichia coli*, Proc. Natl. Acad. Sci. USA 105 (2008) 5537–5542.

[24] A.X. Tran, C. Dong, C. Whitfield, Structure and functional analysis of LptC, a conserved membrane protein involved in the lipopolysaccharide export pathway in *Escherichia coli*, J. Biol. Chem. 285 (2010) 33529–33539.